



King Saud University

Saudi Journal of Biological Sciences

www.ksu.edu.sa  
www.sciencedirect.com



الجمعية السعودية لعلم الحياتة  
SAUDI BIOLOGICAL SOCIETY

ORIGINAL ARTICLE

# Ifosfamide-loaded lipid-core-nanocapsules to increase the anticancer efficacy in MG63 osteosarcoma cells



Sheng-Qun Wang, Qiao Zhang, Chao Sun, Guang-Yao Liu \*

Department of Orthopedics, China-Japan Union Hospital of Jilin University, Changchun, Jilin 130033, China

Received 15 October 2016; revised 27 November 2016; accepted 1 December 2016

Available online 9 December 2016

## KEYWORDS

Osteosarcoma;  
Nanocapsules;  
Ifosfamide;  
Apoptosis;  
Chemotherapy

**Abstract** In this study, we mainly aimed at developing the Ifosfamide-loaded-lipid-core nanocapsules (IFS-LNC) to increase the therapeutic efficacy in osteosarcoma. The nanoparticle was prepared and evaluated in terms of physical, chemical and biological parameters. The lipid-core-nanocapsules were nanosized with narrow particle size distribution and exhibited a high loading capacity. The LNC displayed a sustained release profile of the drug suggesting its potential application in biomedical field and prolonged anticancer therapy. The LNC showed an endocytosis-mediated cellular uptake in MG63 cancer cells which may lead to an accelerated disruption of the acidic endolysosomal vesicles with release of IFS into the cytoplasm. Specifically, IFS-LNC exhibited a significantly higher cytotoxicity than free IFS used at the same concentration. The indiscriminate ability of the drug-loaded formulation increased the apoptosis of cancer cells by increasing the expression levels of caspase-3 and caspase-9 in MG63 cells. Overall, nanoparticulate formulations of Ifosfamide enhanced the therapeutic efficacy in osteosarcoma.

© 2016 The Authors. Production and hosting by Elsevier B.V. on behalf of King Saud University. This is an open access article under the CC BY-NC-ND license (<http://creativecommons.org/licenses/by-nc-nd/4.0/>).

## 1. Introduction

Osteosarcoma is the most common form of bone malignancies in children and adolescents and accounts for 40–80% of

primary skeletal sarcomas (Mankin et al., 1996; Enneking et al., 1980). It frequently occurs in children in first two decades of their life (between 10–25 years of age) (Janeway et al., 2009). Especially, osteosarcoma is more prominent in males than in females. The long cylindrical bones like femur, tibia, and humerus including the knee joint are the main target in osteosarcomas (Fletcher et al., 2002; Schwartz et al., 2007). The standard treatment option for osteosarcoma remains chemotherapy and surgery or combination of both options. For example, surgery alone resulted in 20% of cure while combination with chemotherapy improved the success rate to 70% (Chou and Gorlick, 2006; Schwartz et al., 2007). Despite the increase in the survival rate, 40% of patients on chemotherapy are palliative and toxic and less than 30% of patients are

\* Corresponding author at: Department of Orthopaedics, China-Japan Union Hospital of Jilin University, 176 Xiantai Street, Changchun, Jilin 130033, China. Fax: +86 431 89876922.

E-mail address: [guangyangliu45@yahoo.com](mailto:guangyangliu45@yahoo.com) (G.-Y. Liu).

Peer review under responsibility of King Saud University.



Production and hosting by Elsevier

suffering from recurrent osteosarcoma (Chou and Gorlick, 2006). Therefore, a novel formulation strategy is required to increase the therapeutic efficacy in case of osteosarcoma.

Ifosfamide (IFS), a DNA alkylating agent is one of the widely used antineoplastic drugs. IFS is 3-(2-chloroethyl)-2-[(2-chloroethyl) amino]-tetrahydro-2H-1,3,2-oxazophosphorin-2-oxide and present as white crystalline powder (Pandit and Dash, 2011). IFS is mainly metabolized through CYP 3A4 and CYP 2B6 enzymes. Ifosfamide is used in the treatment of a variety of solid tumors including those of the cervix, endometrium, lung, ovary, testes and thymus as well as in sarcoma and in the treatment of Burkitt's lymphoma (Yang et al., 2015). IFS mainly act by crosslinking DNA strands and inhibits the replication of DNA and leads to cell apoptosis. Despite its potential action, its clinical effect is affected due to its toxicity in the free or natural form (Magnan et al., 2015; Arokiyaraj et al., 2015; Hussain and Hussain, 2015). Moreover it is unstable depending on the pH of the solution. Based on this fact, an effective delivery system is required to protect its activity in the systemic environment (Sorio et al., 2003).

In this regard, lipid-core-nanocapsule (LNC) is non-ionic carriers which have shown great potential as drug delivery systems for topical, oral or systemic applications (Alves et al., 2007; Bernardi et al., 2009). The supramolecular structure of these new carriers has been fully investigated demonstrating that the core is composed of a dispersion of oil and sorbitan monostearate surrounded by the poly(-caprolactone) wall and stabilized by polysorbate 80 (Cruz et al., 2006; Frozza et al., 2010). These particles are able to improve the stability of formulations and exert photoprotective effects. LNCs have increased the biodistribution of trans-resveratrol in different tissues and promoted a significant reduction in the growth of malignant gliomas by increasing intracerebral levels of drug (Jager et al., 2007, 2009). Based on the property of LNC, we expected that upon encapsulation of IFS in LNC, its therapeutic response towards osteosarcoma will be increased.

Taking all of the above considerations into account, the main aim of present study was develop a lipid-core-nanocapsule system to stably protect the Ifosfamide and to increase its anticancer effects. The lecithin and polysorbate 80 will generate negatively charged nanocapsules which were then stabilized by Polycaprolactone polymeric layer. The LNC was characterized for its particle size and release pattern. The anticancer effect of free IFS and drug-loaded formulations was tested in MG63 bone cancer cells. The subcellular distribution of nanocapsules was tested by confocal laser scanning microscope. The apoptosis effect was confirmed by caspase-3 and caspase-9 apoptosis kit.

## 2. Materials and methods

### 2.1. Materials

Poly(-caprolactone) (PCL), sorbitan mono stearate (Span 60®) was purchased from Sigma-Aldrich, China. Lipoid S75 (soybean lecithin) was obtained from Lipoid (Germany). Caprylic/capric triglyceride and polysorbate 80 were purchased from Delaware (Brazil). All other chemicals are of reagent grade and used without further purifications.

### 2.2. Preparation of Ifosfamide-loaded lipid-core-nanocapsule

The lipid core nanocapsule was prepared on the principles of interfacial deposition of pre-formed polymers. The LNC was stabilized by lecithin and polysorbate-80. To prepare drug-loaded LNC, PCL (100 mg), sorbitan monostearate (40 mg), capric triglyceride (12 mg), Ifosfamide (15 mg) was dissolved together in acetone. In parallel, an ethanolic solution (3 ml) containing lecithin (0.03 g) was prepared and poured into the organic phase. The organic mixture was then injected into the aqueous phase containing 80 mg of polysorbate 80 (in 50 ml of water) under constant magnetic stirring at 40 °C. After 10 min, the mixture was subjected to reduced pressure to evaporate the acetone and the remaining solution was concentrated. The final volume was adjusted to 10 ml. The drug loading was evaluated using HPLC method (Shimadzu HPLC (LC 20A Prominence, Shimadzu, Japan). 50 mM of KH<sub>2</sub>PO<sub>4</sub>(pH 5.0) was used as a mobile phase and eluent was detected at 254 nm.

### 2.3. Particle size and zeta potential analysis

The particle size and zeta potential was analyzed using ZetaSizer Nano ZS (Malvern Instruments Ltd., UK). The average diameters were determined after diluting the samples (500×) in ultrapure water. Measurements were taken at 25 °C. All samples were analyzed in triplicate batches (*n* = 3).

### 2.4. Transmission electron microscopy (TEM) image

The morphology and size analysis was performed using transmission electron microscopy (TEM 1200 ExII, JEOL, Tokyo, Japan) operating at 120 kV. The samples were suitably diluted with ultrapure water and placed on a copper grid. Uranyl acetate solution (2% w/v) was used as a negatively-stained control.

### 2.5. In vitro release study

The release profile of IFS from LNC formulation was evaluated by means of dialysis bag method. The release study was performed in PBS and serum media. The serum contains 10% of FBS in RPMI1640 media. The dialysis bags (Spectra Por 7, 10 Kd, Spectrum Laboratories Rancho Dominguez, USA) was used and 1 ml of nanocapsule dispersion was kept in that membrane and sealed from both the sides. The membrane was placed in a 20 ml of release medium containing 2% Tween 80 and kept at 37 °C at constant stirring speed. The sink condition was maintained during the experiment. At predetermined time intervals, 1 ml of the external medium was withdrawn and replaced with fresh medium. The samples were then injected into the HPLC column as mentioned above.

### 2.6. In vitro cytotoxicity assay

MG63 osteosarcoma cells were cultured in RPMI 1640 culture medium supplemented in 10% FBS and 1% penicillin-streptomycin mixture (Balachandran et al., 2015). The cells were maintained at ambient conditions of 5% CO<sub>2</sub> and 95% humidity. The cytotoxicity assay was carried out using MTT assay protocol. Cells were incubated with free IFS and IFS-LNC

and incubated for 24 h. MTT (20  $\mu$ l, 5 mg/ml) was added to each well and incubated with cells for another 4 h. After 4 h, 100  $\mu$ l of DMSO was added to each and the absorbance was measured at 570 nm using a microplate reader (Multiskan, Thermo Fisher, USA). The cells incubate in 6-well plate and treated with respective formulations. The cells were fixed and observed under optical microscope to view the cellular morphology.

### 2.7. Subcellular localization of nanocapsules

MG63 cells were incubated in RPMI 1640 culture medium in a cover slip in 6-well plate and allowed to incubate for 24 h. The rhodamine-B loaded LNC formulation was treated to cells and further incubated for 3 h in the complete culture medium. The media was removed and washed twice with PBS. The cells were then fixed with 4% paraformaldehyde. For intra-nuclear distribution study, DAPI was used for the nucleus staining, and the imaging was processed using confocal laser scanning microscopy (CLSM) (Olympus FV1000, Japan).

### 2.8. Measurement of caspase-3 and caspase-9 activities

Colorimetric assay kits (Sigma–Aldrich) was used to measure the proteolytic activities of caspase-3 and caspase-9. Cells were seeded in 6-well plate at a seeding density of  $1 \times 10^6$  cells/well. Next day, cells were treated with free IFS and IFS-LNC and incubated for 24 h. The cells were extracted and cell pellets were suspended in a lysis buffer in ice for 15 min. The lysate was vortexed and centrifuged and supernatant was collected. 20  $\mu$ l of supernatant was added to a buffer containing a *p*-nitroaniline (pNA)-conjugated substrate for caspase-3 (Ac-DEVDpNA), and (LEHD-pNlabeled) for caspase 9. The cell was incubated for 1 h and the concentration of pNA released was calculated from the absorbance values at 405 nm. Untreated cell was considered as control.

### 2.9. Statistical analysis

Student's *t*-test was used to determine statistical significance. The data are expressed as mean  $\pm$  SD. Two groups were considered statistically significant when  $P < 0.05$ .

## 3. Results and discussion

### 3.1. Characterization of Ifosfamide-loaded nanocapsules

Osteosarcoma is the most common form of bone malignancies in children and adolescents and accounts for 40–80% of primary skeletal sarcomas. The main aim of present study was develop a lipid-core-nanocapsule system to stably protect the Ifosfamide and to increase its anticancer effects. The Ifosfamide-loaded lipid-core-PCL nanocapsules were prepared by interfacial deposition of preformed polymer (Fig. 1). The drug-loaded nanocapsules were characterized in terms of particle size and surface charge. The average particle size of blank as well as drug-loaded nanocapsules was observed to be around  $\sim$ 121 nm and  $\sim$ 136 nm, respectively with an excellent polydispersity index (PDI  $\sim$  0.140). The surface charge of IFS-LNC was observed to be  $-15.4 \pm 0.65$  mV. The negative

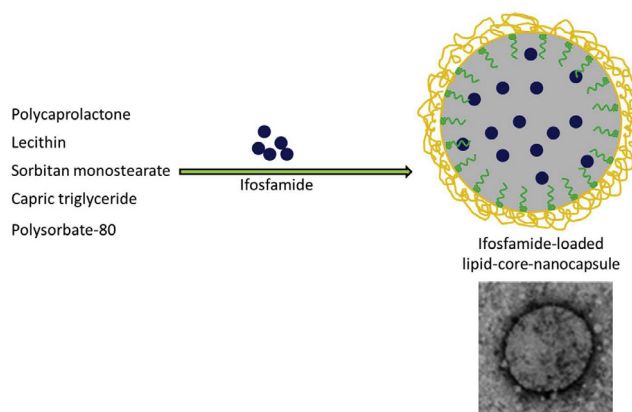


**Figure 1** Schematic illustration of preparation of Ifosfamide-loaded lipid-core-nanocapsules. Insert shows the transmission electron microscope image of lipid-core-nanocapsules.

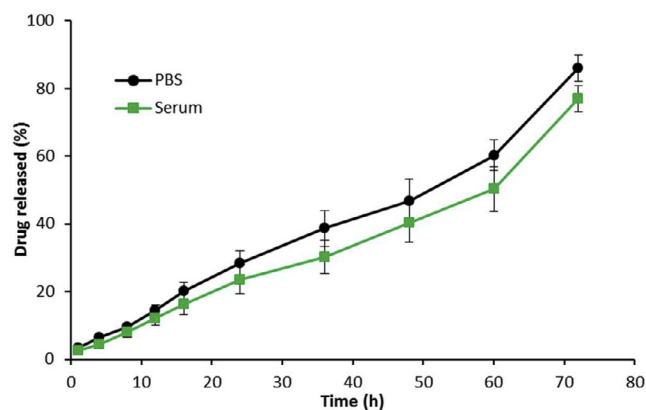


**Figure 2** In vitro drug release profile of IFS from IFC-LNC. The release study was carried out in phosphate buffered saline (PBS) and serum. The study was continued up to 72 h. \* $p < 0.05$  is the statistical difference between release of drug in PBS and ABS.

surface charge was mainly attributed to the presence of lecithin on the lipid structure. Slight increase in particle size was due to the loading of drug in the lipid core. Furthermore, surface charge was slight increased upon loading of the drug. The TEM imaging showed spherical shaped particles with clear core and shell morphology. The entrapment efficiency (EE) was more than 90% indicating its ability to load large quantum of drug and showed a high loading capacity. A high loading capacity is always regarded as best for the cancer targeting or cancer chemotherapeutics.

### 3.2. Drug loading and in vitro drug release study

The IFS-LNC showed a high entrapment efficiency of  $93.25 \pm 1.25\%$  with an active loading capacity of 16.8%. In vitro release of IFS from IFS-LNC was evaluated by means of dialysis method. The release study was performed in phosphate buffered saline (PBS), acetate buffered saline (ABS) and serum to simulate the physiological conditions (Fig. 2). In all the release conditions, IFS released in a controlled and much sustained manner indicating its potential to prolong the blood cir-

ulation after administration in the body. It can be seen that approximately ~26% of IFS released within 24 h of study period. While, nearly 80% of drug released at the end of 72 h of release study. Relatively higher drug release was observed in the acidic conditions. The free IFS completely released within 12 h of study period. Lack of burst release phenomenon further suggests the significant entrapment of drug. Such sustained release of drug indicates that the drug was stably incorporated in the core of nanocapsules. It should be further noted that a controlled release of drug in the serum indicates that much of the drug will be available to get release in the tumor tissues possibly via enhanced retention and permeability (EPR) effect.

### 3.3. Intracellular uptake

In order to assess the possible internalization of nanocapsules, we have performed the cellular uptake experiment using confocal laser scanning microscopy (CLSM) (Fig. 3). Cellular uptake studies provide useful information related to the biocompatibility of novel formulations and its application in drug delivery science. For this purpose, we have stained the nucleus with DAPI (blue color) and drug was replaced with rhodamine-B (red fluorescence). As seen clearly, nanocapsules accumulated in the cytoplasmic region while the nucleus was empty and no red fluorescence was traced. In the merged image, blue fluorescence did not vanish due to the absence of rhodamine-B in the nuclear compartment. The nanocapsules are expected to release the drug in the acidic compartment which will then travel to the nucleus later on with time. This could be attributed to internalization/endocytosis of nanocapsules by the cells. This cytoplasmic compartmentalization profile is in agreement with previous studies (Ramamamy et al., 2014; Choi et al., 2015).

### 3.4. Cytotoxicity assay

The cytotoxic potential of free IFS and IFS-LNC was investigated in MG63 osteosarcoma cancer cells. It can be seen that both the formulations exhibited a typical dose-dependent cytotoxicity in MG63 cancer cells (Fig. 4). Especially, IFS-LNC exhibited a superior anticancer effect compared to that of free IFS across all tested concentrations. IC<sub>50</sub> value was calculated to compare both the formulations quantitatively. The free IFS showed an IC<sub>50</sub> value of 7.12 µg/ml while IFS-LNC showed an effective IC<sub>50</sub> value of 1.08 µg/ml after 24 h incubation. The superior anticancer effect of IFS-LNC was attributed to

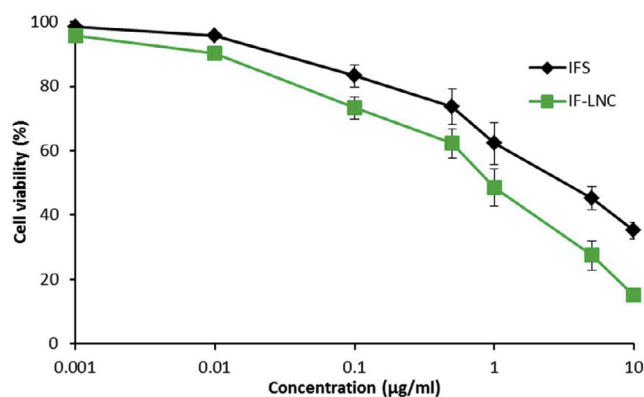


**Figure 4** (a) Cytotoxicity potential of free IFS and IFS-LNC against MG63 osteosarcoma cancer cells; (b) cytotoxicity of blank nanoparticles. The cytotoxicity assay was carried out using MTT assay and presented as percentage cell viability versus concentration of the drugs. \* $p < 0.05$  is the statistical difference between IFS and IFS-LNC.

the sustained release pattern of nanocarrier and endocytosis-mediated cellular uptake in the cancer cell. The blank nanoparticle did not induce any appreciable toxic effect to the cancer cells even when tested at 100 µg/ml. In the clinical setting, we have always faced the problem of dose limitation, defined as the systemic toxicity of conventional chemotherapeutics, an issue that can potentiate the MDR tumor phenotype. Therefore, effective strategy whereby the dose of the drug could be reduced will effectively prevent the side effects of drug. The cytotoxicity assay clearly showed that IFS was very effective in much lower dose when encapsulated in nanocarriers.

### 3.5. Cellular morphology

The cellular morphology of MG63 cancer cells were observed after incubation with respective formulations. The untreated cells maintained their typical morphology and uniformly spread over the entire cover slip (Fig. 5). The IFS treated cells showed sign of apoptosis and the cells were started shrinking and the cell numbers became less. Importantly, IFS-LNC treated cells showed remarkable apoptosis of cancer cells and the cells were rounded and much of the cells were found floating in the incubated media. The cell shrinkage and apoptosis were due to the superior anticancer effect of drug-loaded formulations.

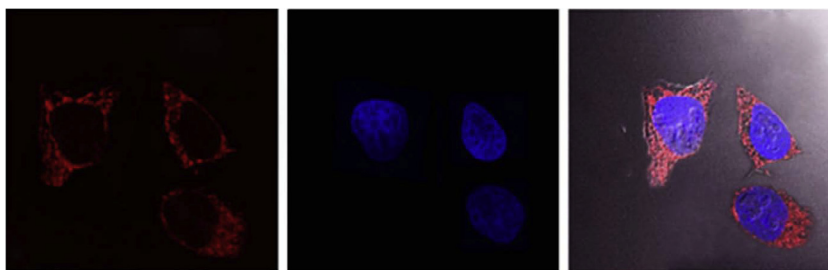


**Figure 3** Confocal microscopic images of uptake of LNC in osteosarcoma cancer cells. The cells are treated with rhodamine-B loaded LNC for 3 h. The nucleus was stained with DAPI while red fluorescence originates from the rhodamine-B.

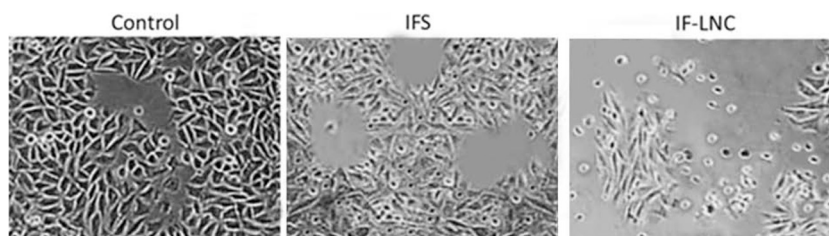


**Figure 5** Bright field microscopic images of MG63 cancer cells. The cells were treated with free IFS and IFS-LNC and incubated for 24 h.

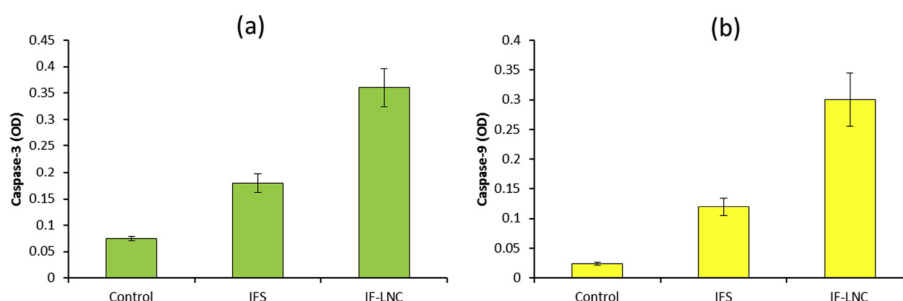


**Figure 6** Caspase-3 and caspase-9 analysis of MG63 osteosarcoma cells. The cells were treated with respective formulations and apoptosis assay was carried out as per the manufacturer's instruction.  $**p < 0.01$  is the statistical difference between free IFS and IFS-LNC.

### 3.6. Apoptosis analysis

In order to assess the specific pathway of apoptosis that was being activated in our system we used a biochemical approach to detect cleavage of caspases 8 and 9, the initiator caspases for the extrinsic and intrinsic pathways of apoptosis respectively (Fig. 6a,b). It has been reported that increase in apoptosis will increase the expression of cell death signaling pathway markers which lead to the over-expression of various caspases (caspase-3 and caspase-9). Especially, caspase-9 triggers the cascade of caspase-apoptosis executors such as caspase-3. In the present study therefore, we have evaluated the level of expression of caspase-3 and caspase-9 upon incubation with different formulations. It can be seen that free IFS induced the expression of both the caspases, however IFS-LNC showed a remarkable increase in the level of caspase-3 and caspase-9. Nearly, two-fold increase in caspases were seen upon incubation with nanoencapsulated IFS. The caspase-3, 9 assay results were consistent with the cytotoxicity assay. Overall, LNC carrier remarkably increased the apoptosis of MG63 osteosarcoma cells than compared to the free IFS indicating its excellent potential to control the cancer progression. Further studies are warranted to prove the therapeutic efficacy of this system in animal models.

## 4. Conclusion

In summary, we have successfully developed unique Ifosfamide-loaded-lipid-core nanocapsules to increase the therapeutic efficacy in osteosarcoma. The lipid-core-nanocapsules were nanosized with narrow particle size distribution and exhibited a high loading capacity. The LNC displayed a sustained release profile of the drug suggesting its potential appli-

cation in biomedical field and prolonged anticancer therapy. The LNC showed an endocytosis-mediated cellular uptake in MG63 cancer cells which may lead to an accelerated disruption of the acidic endolysosomal vesicles with release of IFS into the cytoplasm. Specifically, IFS-LNC exhibited a significantly higher cytotoxicity than free IFS used at the same concentration. The indiscriminate ability of the drug-loaded formulation increased the apoptosis of cancer cells by increasing the expression levels of caspase-3 and caspase-9 in MG63 cells. Overall, nanoparticulate formulations of Ifosfamide enhanced the therapeutic efficacy in osteosarcoma. Further studies are warranted to prove the therapeutic efficacy of this system in animal models.

## Acknowledgement

The study was supported from the funding grant of Jilin University research grant.

## References

- Alves, M.P., Scarrone, A.L., Santos, M., Pohlmann, A.R., Guterres, S. S., 2007. Human skin penetration and distribution of nimesulide from hydrophilic gels containing nano carriers. *Int. J. Pharm.* 341, 215–220.
- Arokiyaraj, S., Saravanan, M., Badathala, V., 2015. Green synthesis of silver nanoparticles using aqueous extract of taraxacum officinale and its antimicrobial activity. *South Indian J. Biol. Sci.* 1, 115–118.
- Balachandran, C., Duraipandian, V., Emi, N., Ignacimuthu, S., 2015. Antimicrobial and cytotoxic properties of streptomyces Sp. (ERINLG-51) isolated from Southern Western Ghats. *South Indian J. Biol. Sci.* 1, 7–14.
- Bernardi, A., Zilberstein, A., Jager, E., Campos, M.M., Morrone, F. B., Calixto, J.B., Pohlmann, A.R., Guterres, S.S., Battastini, A.M.

- O., . Effects of indomethacin loaded nanocapsules in experimental models of inflammation in rats. *Br. J. Pharmacol.* 158, 1104–1111.
- Choi, J.Y., Ramasamy, T., Tran, T.H., Ku, S.K., Shin, B.S., Choi, H. G., Yong, C.S., 2015. Systemic delivery of axitinib with nanohybrid liposomal nanoparticles inhibits hypoxic tumor growth. *J. Mater. Chem. B* 3, 408–416.
- Chou, A.J., Gorlick, R., 2006. Chemotherapy resistance in osteosarcoma: current challenges and future directions. *Expert Rev. Anticancer Ther.* 6, 1075–1085.
- Cruz, L., Soares, L.U., Dalla Costa, T., Mezzalana, G., da Silveira, N. P., Guterres, S.S., Pohlmann, A.R., 2006. Diffusion and mathematical modeling of release profiles from nanocarriers. *Int. J. Pharm.* 313, 198–205.
- Enneking, W.F., Spanier, S.S., Goodman, M.A., 1980. A system for the surgical staging of musculoskeletal sarcoma. *Clin. Orthop.* 153, 106–120.
- Fletcher, C., Unni, K., Mertens, F. (Eds.), 2002. *Pathology and Genetics of Tumours of Soft Tissue and Bone*. IARC Press.
- Frezza, R.L., Bernardi, A., Paese, K., Hoppe, J.B., da Silva, T., Battastini, A.M.O., Pohlmann, A.R., Guterres, S.S., Salbego, C., 2010. Characterization of transresveratrol-loaded lipid-core nanocapsules and tissue distribution studies in rats. *J. Biomed. Nanotechnol.* 6, 694–770.
- Hussain, K., Hussain, T., 2015. Gold nanoparticles: a boon to drug delivery system. *South Indian J. Biol. Sci.* 1, 128–133.
- Jager, A., Stefani, V., Guterres, S.S., Pohlmann, A.R., 2007. Physicochemical characterization of nanocapsule polymeric wall using fluorescent benzazole probes. *Int. J. Pharm.* 338, 297–305.
- Jager, E., Venturini, C.G., Poletto, F.S., Colome, L.M., Pohlmann, J. P.U., Bernardi, A., Battastini, A.M.O., Guterres, S.S., Pohlmann, A.R., 2009. Sustained release from lipid-core nanocapsules by varying the core viscosity and the particle surface area. *J. Biomed. Nanotechnol.* 5, 130–140.
- Janeway, K., Gorlick, R., Bernstein, M., 2009. Osteosarcoma. In: Orkin, S., Fisher, D., Look, A., Lux, S., Ginsburg, D., Nathan, D. (Eds.), *Oncology of Infancy and Childhood*. Saunders Elsevier, Philadelphia, pp. 871–910.
- Magnan, H., Goodbody, C.M., Riedel, E., Pratilas, C.A., Wexler, L. H., Chou, A.J., 2015. Ifosfamide dose-intensification for patients with metastatic Ewing sarcoma. *Pediatr. Blood Cancer* 62, 594–597.
- Mankin, H.J., Mankin, C.J., Simon, M.A., 1996. The hazards of the biopsy, revisited. *Members of the Musculoskeletal Tumor Society. J. Bone Joint Surg. Am.* 78, 656–663.
- Pandit, A.A., Dash, A.K., 2011. Surface-modified solid lipid nanoparticulate formulation for ifosfamide: development and characterization. *Nanomedicine (Lond.)* 6, 1397–1412.
- Ramasamy, T., Kim, J.H., Choi, J.Y., Tran, T.H., Choi, H.G., Yong, C.S., Kim, J.O., 2014. PH sensitive polyelectrolyte complex micelles for highly effective combination chemotherapy. *J. Mater. Chem. B* 2, 6324–6333.
- Schwartz, C.L., Gorlick, R., Teot, L., Krailo, M., Chen, Z., et al, 2007. Multiple drug resistance in osteogenic sarcoma: INT0133 from the Children's Oncology Group. *J. Clin. Oncol.* 25, 2057–2062.
- Schwartz, C.L., Gorlick, R., Teot, L., Krailo, M., Chen, Z., Goorin, A., Grier, H.E., Bernstein, M.L., Meyers, P., 2007. Children's Oncology Group: multiple drug resistance in osteogenic sarcoma: INT0133 from the Children's Oncology Group. *J. Clin. Oncol.* 25, 2057–2062.
- Sorio, R., Lombardi, D., Spazzapan, S., La Mura, N., Tabaro, G., Veronesi, A., 2003. Ifosfamide in advanced/disseminated breast cancer. *Oncology* 65, 55–58.
- Yang, H., Ma, Y., Liu, Z., Wang, Z., Han, B., Ma, L., 2015. Benefit from ifosfamide treatment in small-cell lung cancer: a meta-analysis. *Mol. Clin. Oncol.* 3, 420–424.